

Accentuating the Competency of 3d Transition Metal Doped Mg_4 Clusters towards Molecular Hydrogen Adsorption: A DFT Study

Bishwajit Boruah, Bulumoni Kalita*

Dept. of Physics, Dibrugarh University, Assam, India, 786001

December 21, 2021

Abstract

Density functional theory (*DFT*) studies show that doping of *3dTM* atoms into $Mg_4^{0,+}$ ($TMMg_3^{0,+}$) can alter the endothermic nature of molecular hydrogen adsorption on bare $Mg_4^{0,+}$. H_2 adsorption on $TMMg_3^{0,+}$ clusters depends on the *TM*(*3d*) orbital contribution to the frontier molecular orbitals of the clusters. In $H_2TMMg_3^{0,+}$ complexes, H_2 is adsorbed through donation and back donation of electronic charges with $TMMg_3^{0,+}$ clusters. H_2 binding energy is the maximum for $NiMg_3$ (-0.76 eV) and $FeMg_3^+$ (-0.48 eV) among the neutral and cationic $TMMg_3$ clusters, respectively. The geometry of H_2 adsorption complex entirely depends on the geometry of the host cluster. The lowest energy symmetrical structures of both $NiMg_3$ and $FeMg_3^+$ clusters are less efficient than some slightly higher energy low symmetrical geometrical isomers for adsorption of multiple hydrogen molecules (13.28 H_2 wt% for $NiMg_3$ and 7.89 H_2 wt% for $FeMg_3^+$). Greater exposure of $TM^{0,+}$ along with its lower Mg coordination number make host clusters more suitable for hydrogen storage.

1 Introduction

The present world economy is mostly dependent on the traditional fossil fuels, which take millions of years to form and also releases highly toxic elements into the atmosphere. In such enormously growing demand of energy, hydrogen is possibly the best alternative with its exceptionally impressive mass-energy density and cleanliness. However, to commercialize hydrogen as an energy carrier, its storage medium must fulfil the required gravimetric and volumetric density and fast kinetics set by the Department of Energy (DOE), USA [1]. Accordingly, the necessary binding energy of hydrogen to the storage material should be within the range of 0.1eV- 0.8 eV, which lies in between physisorption and chemisorption [2, 3]. Dissociative chemisorption of hydrogen molecule results in strong metal-hydrogen

*Corresponding Author, bulumonikalita@dibru.ac.in

atom bonds increasing the desorption temperature. This limits the practical application of hydrogen storage. This issue can be resolved through adsorption of hydrogen in its molecular form so that its dissociation on the host material resulting in high chemisorption energy can be avoided. Again, according to the DOE target, the optimum hydrogen storage capacity should be 6.5 wt% for commercial applications [1]. In order to achieve high hydrogen storage capacity, the host material should possess high gravimetric density of hydrogen. This parameter is directly proportional to the number of adsorbed H_2 molecules and inversely proportional to the molecular mass of the host. Therefore, the light elements such as Be, Na, Mg, Al, K and Li due to their reasonably less molecular masses are given importance to achieve high gravimetric density of H_2 for on-board applications [4, 5, 6, 7, 8]. In a previous study on aromatic bimetallic clusters via density functional theory (DFT) calculation, K. Srinivasu and co-workers have reported high gravimetric density of hydrogen in hydrogenated Al_4M_2 , Be_3M_2 , Mg_3M_2 etc (M=Li, Na, K) clusters and proposed the formation of complexes $Al_4M_2(H_2)_{2n}$ and $Be_3M_2(H_2)_{2n}$ by Al_4M_2 and Be_3M_2 clusters through adsorption of multiple hydrogen molecules [7]. Recently Mg based materials have been widely studied to design H_2 storage medium because of their many advantageous properties such as cost effectiveness, abundance, non-toxicity and storage capacity [9, 10, 11, 12, 13, 14, 15, 16, 17, 18, 19]. Yartys et al., in 2019 have reported a very comprehensive review on Mg based hydrogen storage materials including the latest activities, historic overviews and also projecting outlines on future developments putting special importance on improving kinetics and thermodynamic properties [12]. Several theoretical and experimental studies reported that the thermodynamic and kinetics of hydrogen adsorption and desorption can be improved by reducing the size of Mg particles to nanoscale [15, 20, 21, 22]. Jeon et al., in 2011 have been able to adsorb and release hydrogen on Mg nanoparticles below 200 °C [23]. DFT calculations have shown that hydrogen adsorption properties of Mg clusters are tuneable via varying size, charge state, geometry, dopant element, alloying etc [24, 25, 26].]. Effect of transition metal (TM) doping on hydrogen adsorption properties of different host materials is also an interesting area of research [12, 14, 27, 28, 29, 30, 31, 32, 33, 34]. Kubas reported that interaction of H_2 with transition metals takes place via donation of electron from $H_2\sigma$ -orbital to TM vacant d-orbitals followed by back-donation from TM d-orbitals to $H_2\sigma^*$ -orbital, which is famously known as Kubas interaction [35]. However, binding of H_2 varies with different dopant TM as well as with coordination number of the dopant TM in the cluster [12, 14, 27, 28, 29, 30, 31, 32, 33, 34, 35, 36, 37, 38, 39, 40]. Jia et al. highlighted the effect of size dependent Rh+ coordination number in Al_nRh^+ (n=1-12) clusters on hydrogen molecule adsorption. It was reported that lower coordination favours stronger hydrogen binding. Several earlier studies have shown that the catalytic activity of transition metals can greatly improve the hydrogen storage properties of MgH_2 [14, 41, 42]. Xie et al. investigated the hydrogen adsorption properties of MgH_2 nanoparticles doped with Ni nanoparticles and reported that the catalytic effect of Ni can be increased by decreasing the size of the nanoparticle [41]. In another study Cui et al. have explored the hydrogen storage properties of a series of Mg-TM (TM=Ti, Nb, V, Co, Mo, Ni) nanocomposites and ranked the dehydro-

genation performance as $Mg-Ti > Mg-Nb > Mg-Ni > Mg-V > Mg-Co > Mg-Mo$ [42]. Charkin and Maltsev have recently studied the reaction kinetics for the hydrogenation of different 3d transition metal (M) doped $Mg_{17}M$ clusters [43, 44, 45]. They have reported that Ni shows the most favourable reaction kinetics in the formation of $Mg_{17}MH_2$ systems [45]. Trivedi and Bandopadhyay studied the hydrogen adsorption on Rh and Co doped Mg clusters in two different DFT studies and reported Mg_5Co and Mg_9Rh as the most effective hydrogen storage clusters [29, 31]. Ma et al. in another report mentioned that addition of Ti and Nb into Mg_{55} cluster enhances its stability and improve hydrogenation kinetics [33].

In spite of having the advantage of high gravimetric densities, the study on hydrogen adsorption in small clusters of light alkali and alkali-earth metals is highly limited. Next, study on such clusters adsorbing hydrogen in molecular form is even scarcer. However, such studies would be very much useful in designing hydrogen storage materials for practical applications. Motivated by this fact, we intend to make a comprehensive study on the effect of 3d TM doping in Mg_4 cluster towards molecular hydrogen adsorption. In the present study, we have carried out DFT calculations to explore the competency of gas phase 3d TM doped Mg clusters towards molecular hydrogen storage. In this regard, we have investigated various factors governing the process. Accordingly, we have studied the effect of charge states of $TMMg_3$ clusters on molecular hydrogen adsorption; the interplay between the electronic and geometric structures of neutral and cationic $TMMg_3$ clusters as well as their roles in molecular hydrogen adsorption mechanism; nature of adsorption of single and multiple hydrogen molecules on $TMMg_3^{0,+}$ clusters. The results of this study will guide further investigations on molecular hydrogen adsorption properties of small light metal clusters as well as to tune them for completing the search for hydrogen storage materials.

2 Methodology

All calculations have been carried out in the Gaussian 09 package [46] using DFT method. Mg clusters include features of van der Waals interactions and therefore it is important to include dispersion correction in the Mg cluster calculations in a proper way [47]. Moreover, similar treatment is also necessary for studying the physisorption of molecular H_2 in these clusters due to the van der Waals interactions [25]. In a recent article, we have established the reliability of dispersion corrected $\omega B97X-D$ functional for accurate determination of structure and energetics of gas phase small Mgn clusters [47]. $\omega B97X-D$ is a hybrid range-separated functional and capable of capturing both short-range and long-range interactions [48]. The $\omega B97X-D$ method is also reported to be effective in the study of transition metal compounds [49]. Therefore in the present study, we have used $\omega B97X-D$ functional for studying the $H_2Mg_4^{0,+}$ and $(H_2)_nTMMg_3^{0,+}$ complexes formed via adsorption of single and multiple hydrogen molecules on $Mg_4^{0,+}$ and $TMMg_3^{0,+}$ clusters, respectively. 6-311G(d,p) basis set is chosen for Mg and H and LANL2DZ basis set is used for TM atoms. The binding energy per H_2 molecule (E_b) is calculated using the following formula:

$$E_b = \frac{E(H_2TMMg_3^{0,+}) - E(TMMg_3^{0,+}) - nE(H_2)}{n} \quad (1)$$

The capacity of adsorption of multiple hydrogen molecules for the studied clusters is calculated in terms of wt% as given by the following formula:

$$wt\% = \frac{nm(H_2)}{m(TM) + m(3Mg) + m(nH_2)} \quad (2)$$

Here, E, m and n represents total energy of the corresponding complex/cluster, molecular mass and number of corresponding hydrogen molecules.

3 Results and Discussions

3.1 Adsorption of single H_2 molecule on $Mg_4^{0,+}$ and $TMMg_3^{0,+}$ clusters

In a recent study, we have shown that the electronic properties of $TMMg_3^{0,+}$ clusters are mainly governed by $TM^{0,+}(3d)$ orbitals [47]. Therefore, in the present study, we have chosen the $TMMg_3^{0,+}$ clusters along with $Mg_4^{0,+}$ to host the adsorption of molecular hydrogen. Accordingly, we have performed symmetry unrestricted full geometry optimizations via DFT calculations for all possible H_2 adsorption geometries of $Mg_4^{0,+}$ and $TMMg_3^{0,+}$ clusters in different spin multiplicities. It is to be noted that H_2 adsorption on bare $Mg_4^{0,+}$ clusters is an endothermic process (Table A1 in supplementary file (SF)). A previous study with a different computational level has also reported very weak exothermic adsorption of H_2 on Mg_4 cluster [24]. Among the 3d TM series, only doping of V and Ni into Mg_4 could alter its nature of binding with H_2 as shown by the binding energy values of -0.03 eV and -0.76 eV, respectively (Table A1). Therefore, the lowest energy structures of only these two neutral hydrogen adsorption complexes (H_2VMg_3 and H_2NiMg_3) are shown in Figure 1. Increment of binding energy of H_2 after doping of transition metal atoms has also been reported earlier [33]. On the other hand, H_2 binding has been observed to be exothermic in all the doped cationic clusters. The binding energy values of the cationic complexes are presented in Table A2 and they are found to be in the range of -0.01 eV to -0.48 eV. $H_2FeMg_3^{0,+}$ and $H_2VMg_3^{0,+}$ complexes possess the highest and the lowest binding energy of H_2 , respectively. The lowest energy structures of all the $H_2TMMg_3^+$ complexes are also shown in Figure 1. The spin multiplicities of all the lowest energy structures are presented in Figure 1. Structures of all other neutral and cationic complexes are presented in Figure A1 for reference. Almost all the lowest energy $H_2TMMg_3^{0,+}$ complexes carry the structural feature of H_2 being adsorbed on top of the TM, except for $ZnMg_3^+$ (Figure 1). The bond lengths of the stable neutral and cationic clusters are mentioned next to their geometries in Figure 1 (also shown in Table A1 and A2). The $TM - H_2$ bonds in the lowest energy $H_2TMMg_3^{0,+}$ complexes are significantly lower than the $Mg - H_2$ bond in H_2Mg_4 (Table A1). This indicates enhancement in interaction of the hydrogen molecule with the

Mg tetramer due to TM doping. The H_2NiMg_3 complex is found to exhibit the shortest $TM - H_2$ bond length supporting its highest H_2 binding energy value. In H_2NiMg_3 , H-H bond length elongates to 0.84 Å but the average Ni-Mg bond length gets shortened to 2.39 Å from that of 2.61 Å in bare $NiMg_3$ cluster [47]. The $TM^+ - H_2$ bond length values in $H_2TMMg_3^+$ complexes are in the range of 1.84 Å– 3.27 Å and $Zn^+ - H_2$ is found to be the longest bond. The H-H and TM-Mg bond lengths in all the $H_2TMMg_3^+$ complexes are found to be in the range of 0.75 Å– 0.78 Å, 2.58 Å– 3.1 Å, respectively.

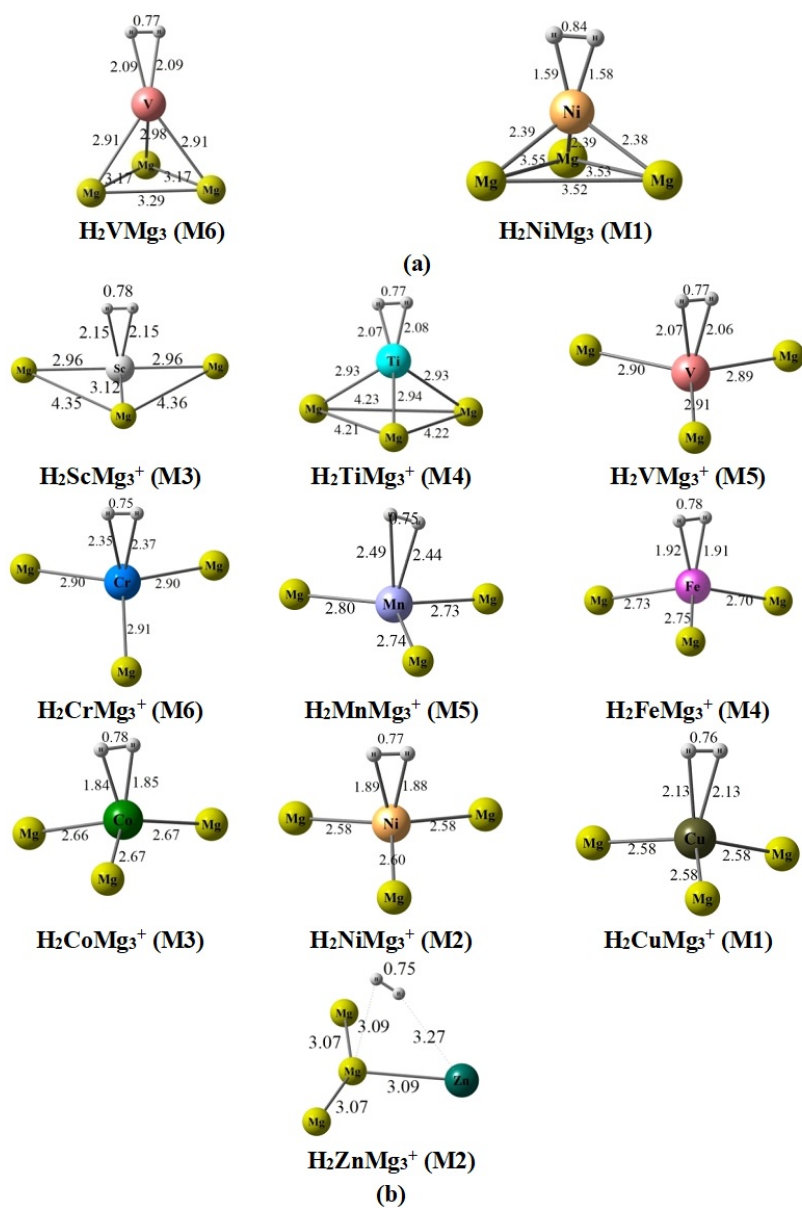


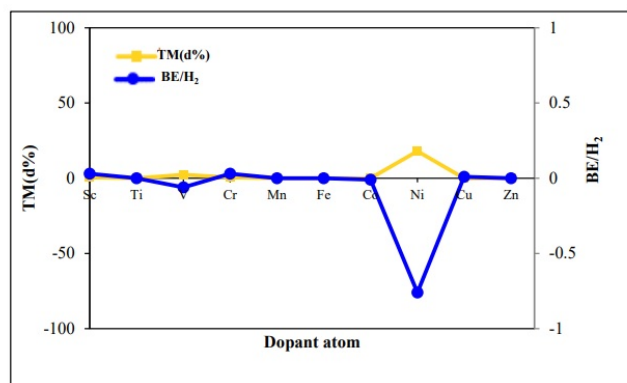
Figure 1: Molecular hydrogen adsorbed (a) H₂TMMg₃ (b) H₂TMMg₃⁺ complexes (bond lengths are in Å). M represents spin multiplicity.

3.1.1 Electronic structures of $TMMg_3^{0,+}$ clusters and adsorption of single H_2 molecule

To explore the nature of interaction of a hydrogen molecule with $TMMg_3^{0,+}$ clusters, we have calculated the percentage of TM(3d) contribution to the HOMO of $TMMg_3^{0,+}$ clusters. These results are based on molecular orbital composition calculations available in Multiwfn software [50]. It is important to mention here that in this calculation, singlet spin state of $NiMg_3$ has only been considered although there is possibility of getting a triplet state too [47]. These two spin singlet and triplet isomers of $NiMg_3$ are almost equally stable with energy difference of only 0.01 eV. The triplet isomer is not found to have any TM(3d) contribution to its HOMO. Moreover, since the most stable H_2NiMg_3 complex exists in singlet spin state (section 3.1) and also the other $TMMg_3^{0,+}$ clusters retain their spin states in their corresponding $H_2TMMg_3^{0,+}$ complexes, we have considered the singlet state electronic structure of $NiMg_3$ cluster to study molecular hydrogen interaction. This validity of this argument is justified by the range of H_2 binding energies that is reasonably smaller than the chemisorption process (section 3.1) and hence it is unlikely that the spin state of the cluster may get changed after formation of $H_2TMMg_3^{0,+}$ complexes. Further analyses to be presented in the following discussion will provide more insight into this aspect. We have plotted the calculated values of percentage contribution of TM(3d) towards the HOMO of $TMMg_3^{0,+}$ clusters with the H_2 binding energies (BE) in the $H_2TMMg_3^{0,+}$ complexes and have presented in Figure 2. This figure clearly indicates that the binding energy of molecular hydrogen in $H_2TMMg_3^{0,+}$ complexes is a direct consequence of the TM(3d) orbital contribution to the HOMOs of the host $TMMg_3^{0,+}$ clusters. This is due to the fact that presence of TM(3d) orbitals in the HOMOs of the host cluster favours H_2 binding with the TM atoms of the cluster via Kubas interaction [35]. Figure 2(a) shows that except for VMg_3 and $NiMg_3$, the TM(3d) contribution in HOMO of all the other clusters is absent making molecular hydrogen adsorption unfavourable in these clusters. Interestingly, electron deficiency in the cationic clusters pushes their HOMOs down in energy with reference to the neutral clusters, which make them capable of getting contributed from the TM(3d) orbitals. This shifting of HOMO levels in $TMMg_3^+$ clusters was already shown in the density of states (DOS) analysis in our previous study [47]. $ZnMg_3^+$, although an exception in this regard, exhibits exothermic nature of binding with H_2 . However, H_2 binding energy with $ZnMg_3^+$ is the lowest among the cationic clusters, which supports the largest bond length value of $Zn^+ - H_2$ as discussed above.

3.1.2 Adsorption mechanism of single H_2 molecule on $NiMg_3$ cluster

To study the interaction mechanism of H_2 with the host clusters, we have performed natural bond orbital (NBO) and density of states (DOS) calculations. The results of NBO calculations derived from Gaussian 09 have been utilized to interpret the interaction of frontier molecular orbitals of the H_2 molecule and the clusters. The DOS calculations are carried out separately in Multiwfn software. Since hydrogen binding is found to be the maximum in H_2NiMg_3 complex, we are now going to discuss the interaction mechanism of hydrogen



(a)

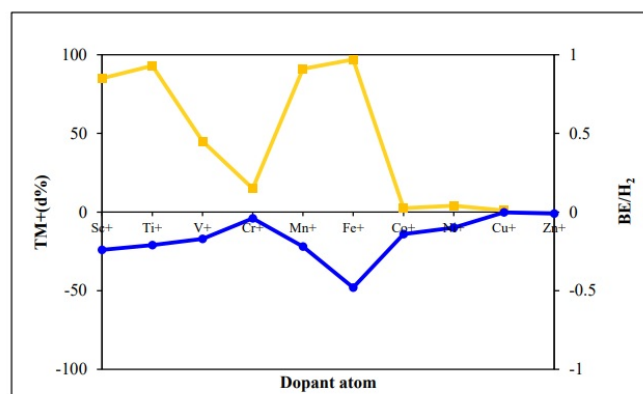


Figure 2: Molecular hydrogen adsorbed (a) H_2TMMg_3 (b) $H_2TMMg_3^+$ complexes (bond lengths are in Å). M represents spin multiplicity.

molecule with $NiMg_3$ cluster considering the most stable geometry of the complex. The results for the rest of the neutral and cationic complexes are provided in the SF (Table A3-A6 and Figure A2-A5). In Figure 3, we have shown a schematic representation of the interaction of the frontier molecular orbitals of H_2 and $NiMg_3$ cluster as obtained from the molecular orbital analysis. According to perturbation theory, the interaction of HOMO (filled orbital) of one system with LUMO (empty orbital) of another can lead to overall stabilization through donor-acceptor bonding interaction[3]. It is observed that the HOMO of H_2 having energy -14.10 eV interacts with the LUMO of $NiMg_3$ with energy (-0.83 eV) resulting in more stable bonding orbitals of the H_2NiMg_3 complex (-15.42 eV). Similarly, HOMO (-6.16 eV), HOMO-1 (-6.17 eV) of $NiMg_3$ interact with the LUMO of H_2 (-3.78 eV) forming H_2NiMg_3 bonding orbitals of energies -6.42 eV and -7.61 eV. Therefore, interaction of H_2 molecule with $NiMg_3$ is mediated via the Ni atom and the interaction takes place due to donation and back donation of electronic charges, i.e., the Kubas interaction [35]. Further, careful observation of the donor-acceptor data of NBO results for H_2NiMg_3 (Table 1) reveals the presence of additional interaction in the complex arising from some of the molecular orbitals not included in Figure 3(a). Significant values of second order energy correction (E(2)) in Table 1 suggests interactions of H_2 bonding orbital (BD) with spd hybridised orbital of Ni (LP*) as well as H_2 anti-bonding orbital (BD*) with Ni(3d) (LP). These interactions are also confirmed from the partial density of states (PDOS) analysis shown in Figure 3(b). The PDOS plots clearly show the presence of interactions between H_2 and Ni in H_2NiMg_3 at various energy scales. The corresponding energies are precisely evaluated as -15.42 eV, -8.5 eV, -7.61 eV and 6.42 eV in consultation with the molecular orbital analyses to be provided in section 3.2.1. Similar type of interactions are also seen in other $H_2TMMg_3^{0,+}$ complexes except for $H_2ZnMg_3^+$ (Figure A2-A3 in SF). $H_2ZnMg_3^+$ is survived with weak van der Waals type interaction rather than the Kubas interaction. This observation is consistent with that discussed earlier in the beginning of section 3.1.

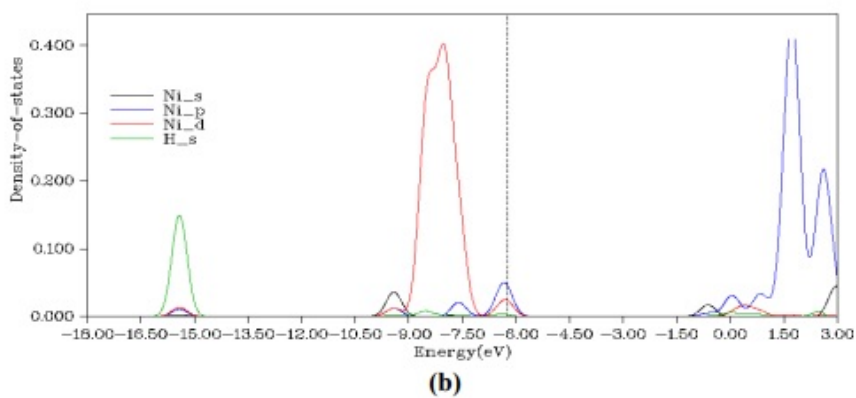
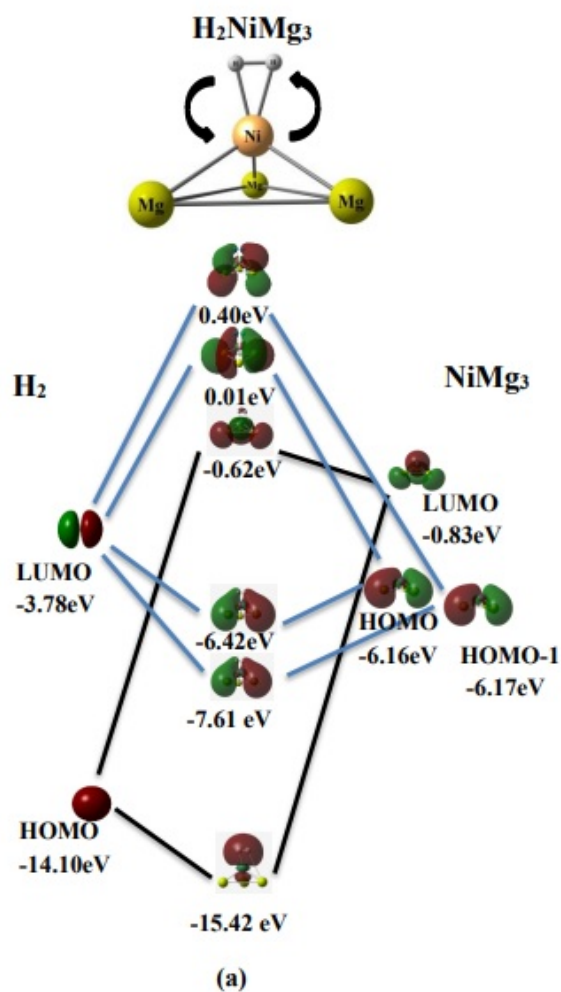


Figure 3: (a) Schematic representation of the interaction of the frontier molecular orbitals of H_2 and NiMg_3 cluster (b) PDOS plots of H_2NiMg_3 complex.

Table 1: Donor acceptor analysis of H_2NiMg_3 complex. E(2) represents the second order energy correction.

H_2NiMg_3	
Donor	Acceptor
BD (H – H)	LP* (Ni) s (34.48%) p 1.72 (59.23%) d 0.18 (6.29%),E(2) = 4.52 eV
LP (Ni) s (2.58%) p 1.43 (3.70%) d 36.28 (93.72%)	BD* (H – H),E(2) = 1.21 eV

3.2 Adsorption of multiple H_2 molecules on $TMMg_3^{0,+}$ clusters

Now, we are going to find the capacity of the $TMMg_3^{0,+}$ clusters in adsorbing multiple H_2 molecules, which will be parameterized by the gravimetric density calculations. The gravimetric density is considered as a key attribute of an efficient hydrogen storage material and it is represented as %wt (equation number (2)) of hydrogen adsorbed by the material. Higher the value of %wt of H_2 , higher will be the gravimetric density and hence efficiency of a material in adsorbing H_2 . In the section 3.1., $NiMg_3$ and $FeMg_3^+$ have been confirmed as the most efficient neutral and cationic $TMMg_3$ clusters for adsorption of single H_2 molecule. Therefore, we are now going to examine the capacity of these clusters in adsorbing multiple H_2 molecules within the optimum binding energy range of 0.1 eV – 0.8 eV per H_2 molecule as mentioned in the introduction.

3.2.1 Adsorption of multiple H_2 molecules on $NiMg_3$ cluster

$NiMg_3$ clusters adsorbing n number of H_2 molecules will be represented as $(H_2)_nNiMg_3$ complexes and the corresponding lowest energy optimized structures are shown in Figure 4(a). First, we have performed the geometry optimization for the $(H_2)_nNiMg_3$ complexes through stepwise addition of H_2 molecules to the lowest energy tetrahedral structure of H_2NiMg_3 shown in Figure 1(a). The binding energy per H_2 molecule (BE/ H_2) is found to decrease gradually with the number of hydrogen molecules (-0.76 eV – -0.10 eV). Ultimately, six numbers of H_2 in total could get adsorbed on $NiMg_3$ cluster within the required binding energy range. It is noticeable in Figure 4(a) that the first H_2 molecule maintains its position on-top of $NiMg_3$ even after successive addition of further five numbers of H_2 . It is also obvious that the interactions of five out of the six H_2 molecules are taking place only in one side of $NiMg_3$, i.e., towards the Ni atom site. Based on these two factors, it has been realized that the position of the first H_2 molecule as well as the compact three-dimensional geometry of the host may be responsible for creating congestion among multiple H_2 molecules hindering the process from continuing further. We have therefore become more curious to know about the effect of geometry of the host cluster on its hydrogen gravimetric density. Accordingly, we have next considered the planar geometry (P) of $NiMg_3$ cluster, which has already been reported in our previous study as a stable isomer of $NiMg_3$ with

only 0.6 eV higher in energy than the most stable tetrahedral (T) $NiMg_3$ isomer [47]. Figure 4(b) shows the optimized structures of $(H_2)_n NiMg_3$ complexes in the $NiMg_3$ (P) isomer. The binding energy variations with number of H_2 molecules for the T and P isomers are compared in Figure 5. Interestingly, BE/H_2 in P isomer slightly increases for the second H_2 and starts decreasing gradually thereafter. The factors affecting the distinguishing behaviour of the T and P isomers towards adsorption of multiple H_2 molecules will be discussed in the following section. It is also observed that in the planar geometry, $NiMg_3$ cluster can adsorb up-to ten hydrogen molecules within the optimum binding energy range. The calculated wt% values of H_2 in the T and P isomers of $NiMg_3$ are found to be 8.42 and 13.28, respectively. This clearly confirms our intuition that the geometry of the host cluster plays a crucial role in governing the adsorption of multiple hydrogen molecules in small clusters.

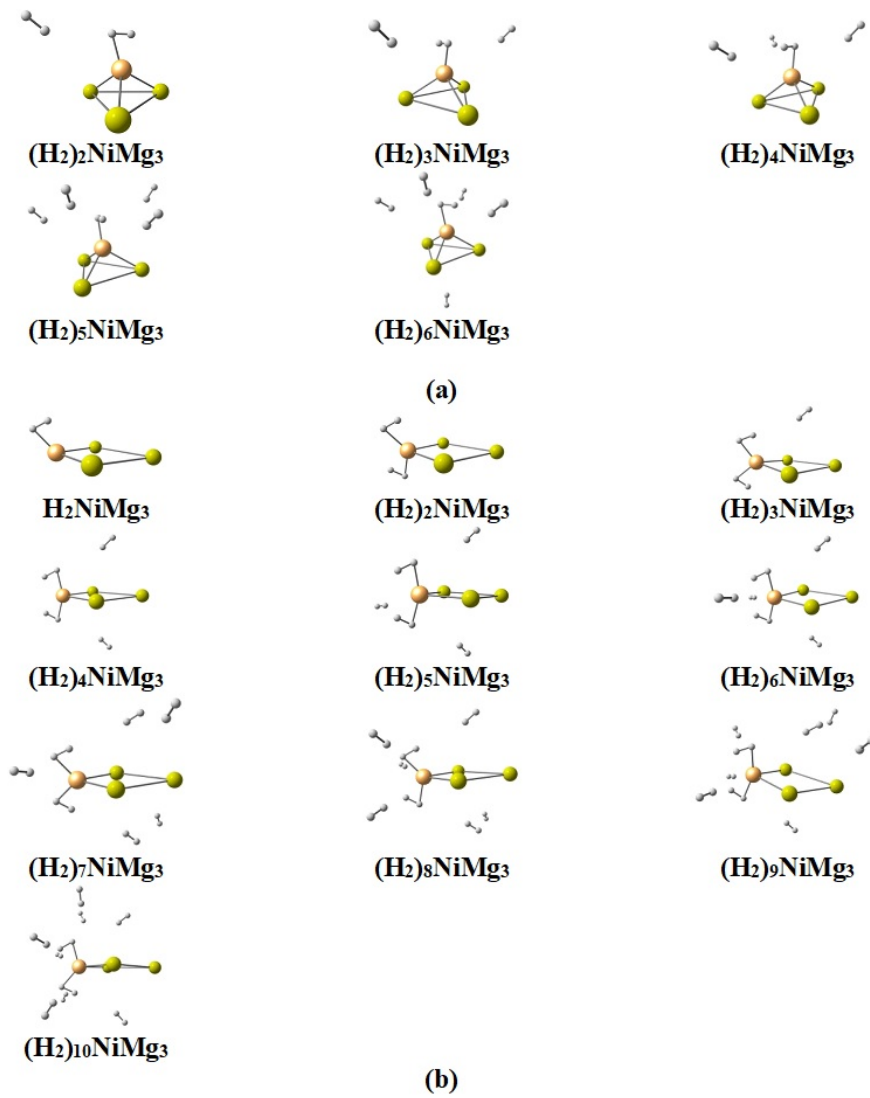


Figure 4: Multiple H_2 adsorption on (a) tetrahedral (T) and (b) planar (P) isomer of NiMg_3 cluster.

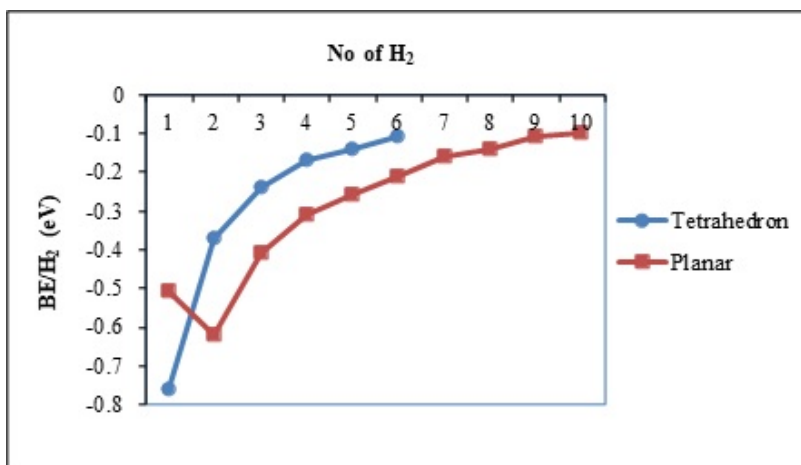


Figure 5: : Variation of BE/ H_2 with no of H_2 on tetrahedral and planar isomer of $NiMg_3$ cluster.

3.2.1.1 Adsorption mechanism of multiple H_2 molecules on structural isomers of $NiMg_3$ cluster

3.2.1.1.1 Electron density distribution and adsorption of multiple H_2 molecules

We have just seen that the planar isomer of $NiMg_3$ can accommodate larger number of H_2 molecules than the tetrahedral isomer. Moreover, there is a distinct jump in H_2 binding energy while going from the first to third H_2 molecule (Figure 5) in P isomer. This behavioural difference between T and P isomers of $NiMg_3$ can be explained from careful investigation of their geometrical and electronic structures. It is observed that the adsorption site for the first H_2 is not similar in the T and P isomers, which affect the adsorption mode of the second H_2 . Figure 6 shows the electrostatic potential (ESP) surface plots of these isomers before and after adsorption of H_2 . The red and blue colours represent the electronegative and electropositive surfaces, respectively. The upper panel in Figure 6(a) presents the ESP surfaces of T isomer of $NiMg_3$ cluster before H_2 adsorption. Here, the electronegative surfaces are observed around Ni–Mg bonds indicating the presence of electron density. In the same isomer, the electropositive surfaces are observed on Ni as well as all the Mg atoms. Due to adsorption of H_2 molecule on top of the Ni atom in T isomer, the electron density existing over the Ni–Mg bonds gets delocalized and reduce the electropositive surface on Ni atom as seen from the lower panel of Figure 6(a). As a result of this, it becomes difficult for the next H_2 to reach and interact with Ni atom in T isomer. Therefore, the second H_2 is not capable to alter the position of the first and hence electronic structure of the adsorption complex with only the first H_2 molecule is retained in the T isomer. Because of this, the adsorption configuration and the associated electronic structure of H_2NiMg_3 complex become effective in controlling the adsorption

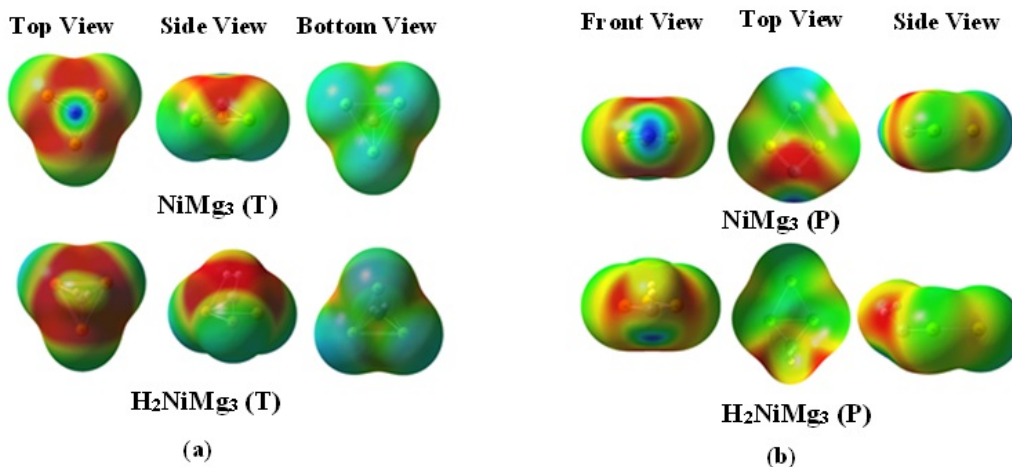
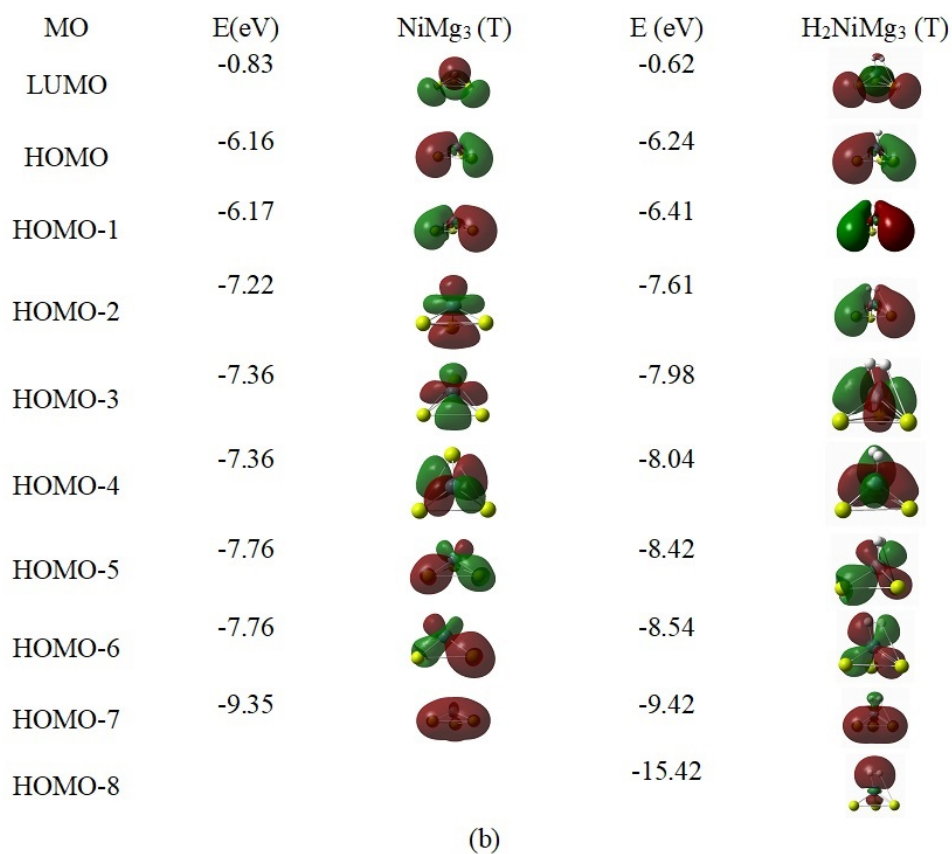
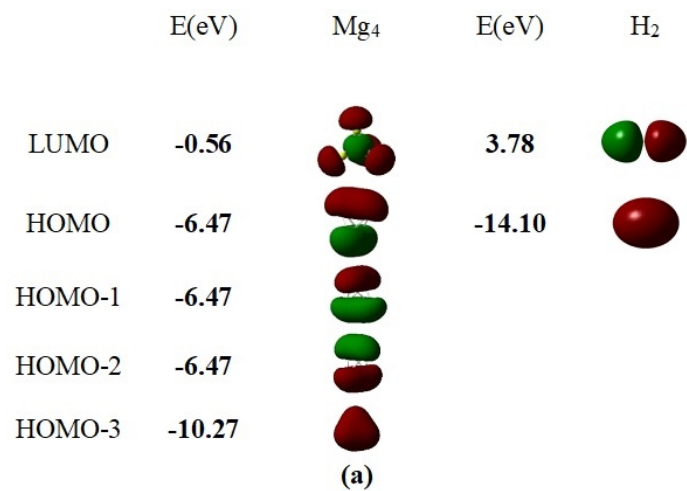


Figure 6: Electro static potential (ESP) plots of T and P isomers of NiMg_3 cluster before and after adsorption of H_2 .

geometry as well as strength of interaction for successive hydrogen molecules. That is why, the binding energies decrease with increasing number of H_2 molecules (Figure 5). In the P isomer, the electronegative surfaces are observed around Ni–Mg and Mg–Mg bonds whereas electropositive surfaces localize over Ni as well as all of the Mg atoms before H_2 adsorption (upper panel of Figure 6(b)). In this isomer, the first H_2 is adsorbed on the Ni atom in a tilted geometry, which could provide ample opportunity to the next H_2 molecule to approach the Ni atom and interact with it. The ESP plots for P isomer after the first H_2 adsorption (lower panel in Figure 6(b)) shows that the electropositive surface from the top of Ni atom shifts towards its side opposite to the adsorbed H_2 molecule. This new position of the electropositive surface actually facilitates the adsorption of the second H_2 . It is important to note here that the second H_2 molecule also acquires a tilted geometry making further adsorption of H_2 favourable. This process could therefore ultimately result in adsorption of a reasonably higher number of H_2 molecules in NiMg_3 cluster in its planar isomer than that in the tetrahedral isomer.

3.2.1.1.2. Molecular orbital analysis and adsorption of multiple H_2 molecules

Figure 7(b) and 7(c) show the molecular orbitals (MOs) of T and P isomers of $NiMg_3$ cluster before and after adsorption of single H_2 molecule. The MOs of bare Mg_4 and the H_2 molecule are also shown in Figure 7(a) for comparison. We can see here that the positive and negative iso-surfaces of the frontier MOs in Mg_4 are very well separated in contrast with those in $NiMg_3$. Such separation prohibits the interaction of Mg_4 with molecular hydrogen. However, presence of Ni(3d) orbital contribution in the frontier MOs of $NiMg_3$ isomers (section 3.1.1. and Figures 7(b) and 7(c)) changes their shapes and reduces the separation between the positive and negative iso-surfaces at the Ni atom site. Due to this, the H_2 molecule is captured by the $NiMg_3$ isomers on top of Ni between the two iso-surfaces. Further, orientations of the MOs in $NiMg_3$ cluster (HOMO and HOMO-1 in T isomer; HOMO, HOMO-1 and HOMO-2 in P isomer) also indicate their possible interactions with the LUMO of H_2 molecule. Such interactions constitute the MOs (HOMO-1, HOMO-2) of H_2NiMg_3 complex corresponding to the T isomer of $NiMg_3$ (Figure 7(b)). In this complex, the HOMO-6 orbital shows mixing of Ni 3dxz orbital with H_2 (LUMO). Similarly, the HOMO-7 and HOMO-8 orbitals of the same complex are due to the interaction of H_2 bonding orbital with the LUMO of $NiMg_3$ (T). In P isomer of $NiMg_3$, Ni(3d) orbitals in the xy plane combine with Mg orbitals and forms jellium type orbitals (HOMO, HOMO-1 of $NiMg_3$ (P) in Figure 7(c)), whereas 3d orbitals in xz and yz planes remain isolated (HOMO-2 of $NiMg_3$ (P) in Figure 7(c)). In the H_2NiMg_3 (P) complex, the H_2 bonding orbital mixes with the LUMO of $NiMg_3$ (P) and gives rise to HOMO-1, HOMO-7 and HOMO-8 orbitals of the complex (Figure 7 (c)). On the other hand, H_2 (LUMO) interaction with Ni(3dxz) orbital forms the HOMO-6 orbital of H_2NiMg_3 (P), whose orientation compels the H_2 molecule to get adsorbed only on one side of Ni in the complex helping the next hydrogen to interact from the opposite side.



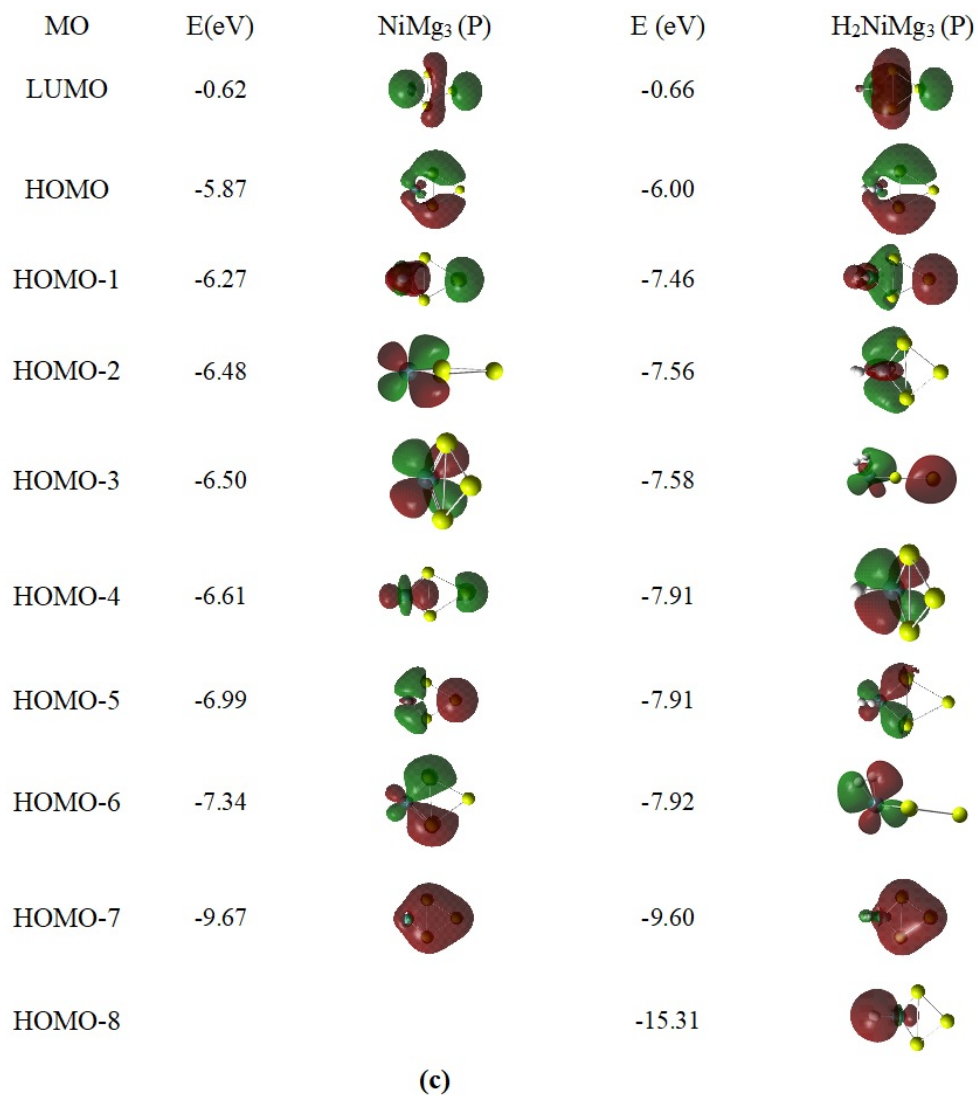


Figure 7: Molecular orbitals of (a) Mg₄ and H₂ (b) NiMg₃/H₂NiMg₃ (T) (c) NiMg₃/H₂NiMg₃ (P) complexes.

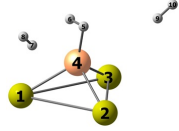
3.2.1.1.3. Charge transfer and adsorption of multiple H_2 molecules

Table 2 shows the natural electronic configurations of $(H_2)_nNiMg_3$ ($n=1-3$) complexes along with those of bare $NiMg_3$ isomers. The corresponding data for the rest of the complexes are provided in the SF (Table A7). The computed electronic configurations for free Mg and Ni atoms are found to be Mg [core]3s(2.00) and Ni [core]4s(1.25)3d(8.74), respectively. With reference to these, Ni(4s) orbital in the lowest energy $NiMg_3$ (T) cluster has been observed to donate electronic charge to all the Mg atoms and gain significant electron density in its 4p and 3d orbitals. The Mg atoms loss electron density from their 3s orbitals and gain in 3p orbitals. The electronic configurations of all the Mg atoms in the T isomer are identical, which signifies equivalent nature of interaction between each of them and the Ni atom (Table 2). Charge transfer process in P isomer involves similar set of molecular orbitals of Ni and Mg as that of T isomer. However, the mechanisms are different in various ways. The overall gain in electron density by Ni in the P isomer is less compared to that in T isomer. Unlike T isomer, only the Mg atoms sitting near to Ni in P isomer (Mg1 and Mg2) participate in the charge transfer process. Moreover, the gain in charge density in the 3p orbitals of the two interacting Mg atoms in P is almost three times higher than that of each Mg atom in isomer T. The Mg atom away from Ni (Mg4), in exception, is found to have non-equivalent electronic configuration with comparatively less change in its electron density than the other two Mg atoms. After adsorption of the first H_2 molecule, there are much higher charge gain and lower charge loss in Ni(4p) and Ni(4s) orbitals, respectively, in isomer T than those in isomer P (Table 2). As a result of this, the resultant gain in electron density by Ni atom in the T is more than that in the P isomer. This property helps in strengthening the interaction of single hydrogen molecule with T isomer of $NiMg_3$ over the P isomer. The higher electron withdrawal nature of Ni in H_2NiMg_3 (T) complex can be attributed to its isotropic Mg environment, where all the three Mg atoms retain their equivalent electron density distributions rendering their equal participations in H_2 adsorption. As expected, the Mg1 and Mg2 atoms in H_2NiMg_3 (P) complex carry similar charge distributions but the isolated Mg4 atom behaves in a totally different way. This also confirms the unequal participations of the Mg atoms in the planar geometry of H_2NiMg_3 complex making its interaction with H_2 relatively less strong than the tetrahedral geometry. The donor acceptor interaction for the second H_2 in $(H_2)_2NiMg_3$ (T) is found to be weak resulting in insignificant changes of electronic charges in the corresponding Ni (4p) and Mg(3s) orbitals. Interestingly, in spite of relatively weaker interaction for the first hydrogen molecule in H_2NiMg_3 (P), Ni atom in $(H_2)_2NiMg_3$ (P) complex gains significant electrons in its 4p orbital accompanied by very little electron loss from the 3s orbitals of Mg1 and Mg2. Therefore, we can say that the suppressed interaction in H_2NiMg_3 (P) is favourable for interaction with the second H_2 molecule. But stronger interaction in H_2NiMg_3 (T) is responsible for its inert nature towards the next H_2 molecule. Both these cases, however, exhibit weaker donor acceptor interactions for further addition of H_2 molecules and hence their BE/H_2 values have similar decreasing trends afterwards (Figure 5).

Table 2: Natural electronic configurations of NiMg₃ isomers and their H₂ adsorbed complexes (atom numbers are provided for reference).



NiMg₃ (T)



(H₂)₃NiMg₃ (T)

T

Mg1 3S(1.40)3p(0.13)3d(0.01)4p(0.01)
Mg2 3S(1.40)3p(0.13)3d(0.01)4p(0.01)
Mg3 3S(1.40)3p(0.13)3d(0.01)4p(0.01)
Ni4 4S(0.67)3d(9.70)4p(0.98)5p(0.01)

Mg1 3S(1.29)3p(0.15)4p(0.01)
Mg2 3S(1.29)3p(0.15)4p(0.01)
Mg3 3S(1.29)3p(0.15)4p(0.01)
Ni4 4S(0.63)3d(9.62)4p(1.49)5p(0.01)
H5 1S(0.94)
H6 1S(0.94)

Mg1 3S(1.29)3p(0.15)4p(0.01)
Mg2 3S(1.29)3p(0.15)4p(0.01)
Mg3 3S(1.29)3p(0.15)4p(0.01)
Ni4 4S(0.63)3d(9.62)4p(1.51)5p(0.01)
H5 1S(0.94)
H6 1S(0.94)2S(0.01)
H7 1S(1.00)
H8 1S(0.99)

Mg1 3S(1.28)3p(0.15)4p(0.01)
Mg2 3S(1.26)3p(0.15)4p(0.01)
Mg3 3S(1.29)3p(0.15)4p(0.01)
Ni4 4S(0.63)3d(9.62)4p(1.54)5p(0.01)
H5 1S(0.94)
H6 1S(0.94)2S(0.01)
H7 1S(0.99)
H8 1S(1.00)
H9 1S(0.99)
H10 1S(1.00)



NiMg₃ (P)



(H₂)₃NiMg₃ (P)

P

NiMg₃

Mg1 3S(1.44)3p(0.36)3d(0.01)4p(0.01)
Mg2 3S(1.44)3p(0.36)3d(0.01)4p(0.01)
Ni3 4S(0.65)3d(9.65)4p(0.16)5S(0.01)5p(0.01)
Mg4 3S(1.65)3p(0.22)4S(0.01)

H₂NiMg₃

Mg1 3S(1.47)3p(0.28)4p(0.01)
Mg2 3S(1.47)3p(0.28)4p(0.01)
Ni3 4S(0.49)3d(9.59)4p(0.40)5p(0.08)
Mg4 3S(1.74)3p(0.16)
H1 1S(1.02)2S(0.01)
H2 1S(0.98)2S(0.01)

(H₂)₂NiMg₃

Mg1 3S(1.39)3p(0.25)4p(0.01)
Mg2 3S(1.39)3p(0.25)4p(0.01)
Ni3 4S(0.49)3d(9.54)4p(0.92)
Mg4 3S(1.75)3p(0.15)
H5 1S(0.96)
H6 1S(0.95)
H7 1S(0.96)
H8 1S(0.95)

(H₂)₃NiMg₃

Mg1 3S(1.37)3p(0.27)4p(0.01)
Mg2 3S(1.37)3p(0.27)4p(0.01)
Ni3 4S(0.49)3d(9.54)4p(0.92)
Mg4 3S(1.72)3p(0.17)
H5 1S(0.95)
H6 1S(0.95)
H7 1S(0.95)
H8 1S(0.96)
H9 1S(1.00)
H10 1S(0.99)

3.2.2 Multiple H_2 adsorption of $FeMg_3^+$

Among the cationic clusters, $FeMg_3^+$ possesses the highest binding energy for single H_2 adsorption. Therefore, we have checked the multiple H_2 adsorption capacity of this cationic cluster only and accordingly calculated the H_2 wt% for it. So far, we have seen that the structural geometry of $NiMg_3$ isomers governs the multiple H_2 adsorption process for the cluster. With the same logic, we have decided to proceed with two different structural isomers of $FeMg_3^+$. In this regard, the most stable isomer of $FeMg_3^+$ (Isomer I) along with another one (Isomer II) with 0.16 eV higher in energy are considered. In these two isomers, subjection of Fe^+ is different as shown in Figure 8. Calculations reveal that the isomer II can adsorb up to five H_2 molecules (7.26 wt% H_2) against maximum of four H_2 molecules in isomer I (5.89 wt% H_2) within the optimum binding energy range of 0.1-0.8 eV. The evolutions of binding energy per H_2 molecule for $FeMg_3^+$ isomers are shown in Figure 9. It is seen here that the relatively higher BE value for the first H_2 molecule in Isomer I is not capable of keeping it competent for multiple H_2 adsorption. This is in consistent with that observed for $NiMg_3$ isomers. Actually, position of Fe^+ in Isomer II is more suitable than that in Isomer I for interaction with the H_2 adsorbate. This configuration in Isomer II is maintained even after successive H_2 adsorption. The nature of the electrostatic potential surfaces for the $FeMg_3^+$ isomers before and after H_2 adsorption (Figure A6 in SF) are similar to those of $NiMg_3$ isomers as discussed in section 3.2.1.2. Moreover, analyses of the other electronic properties such as the molecular orbitals and the charge transfer processes in $FeMg_3^+$ isomers before and after H_2 adsorption also follows the explanations of those in $NiMg_3$ isomers. The molecular orbitals and electronic configurations of bare and hydrogen adsorbed $FeMg_3^+$ isomers are provided in Figure A7 and Table A8 in the SF. On the basis of these various parameters, it is confirmed that the cluster geometry irrespective of its charge state can dictate the nature of hydrogen adsorption and thereby govern the gravimetric density of the cluster for storage of molecular hydrogen.

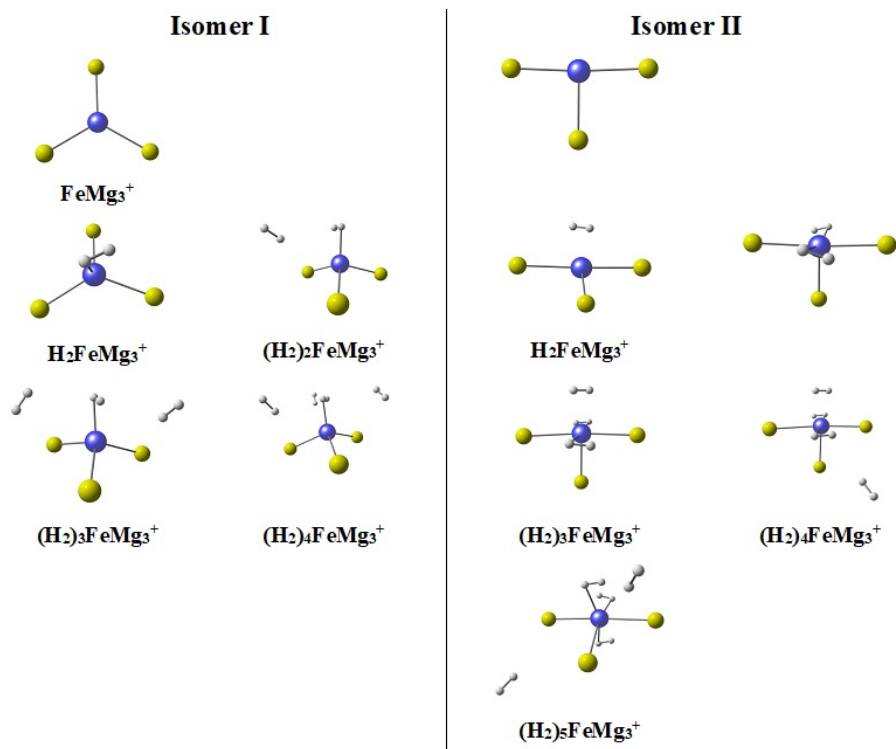


Figure 8: Multiple H_2 adsorbed complexes of FeMg_3^+ isomers.

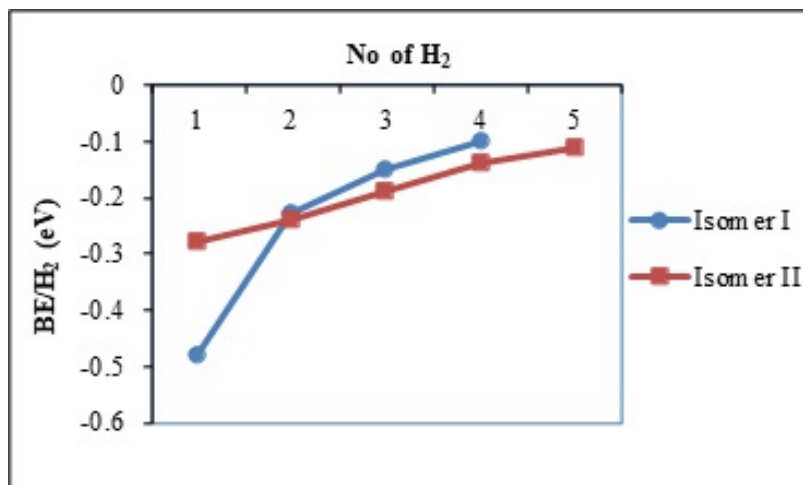


Figure 9: Variation of binding energy per H_2 molecule (BE/H_2) with number of H_2 on Isomer I and isomer II of FeMg_3^+ cluster.

4 Conclusion

We have investigated the molecular hydrogen adsorption properties of $TMMg_3^{0,+}$ clusters. It has been found that doping of 3d TM atoms into $Mg_4^{0,+}$ clusters convert the molecular hydrogen adsorption process in the clusters from endothermic to exothermic nature. Hydrogen binding with $TMMg_3^{0,+}$ clusters is dependent on the TM(3d) orbital contributions of the clusters to their frontier MOs. Molecular H_2 is adsorbed in $TMMg_3^{0,+}$ clusters through donor acceptor interaction. It has also been observed that shifting of HOMO positions towards lower energy in $TMMg_3^+$ clusters increase their TM(3d) orbital contributions in the HOMOs. This leads to enhancement of H_2 binding energies in cationic $TMMg_3$ clusters from their neutral counterparts. That is why exothermic H_2 adsorption takes place in all $TMMg_3^+$ clusters in contrast with only VMg_3 and $NiMg_3$ among the neutral clusters. Adsorption energy for single H_2 is found to be the maximum for $NiMg_3$ (-0.76 eV) and $FeMg_3^+$ (-0.48 eV) clusters. Based on these results, we can suggest TM(3d) orbitals participation in the HOMOs of the host $TMMg_3^{0,+}$ clusters as the necessary criterion for molecular hydrogen adsorption and this property can be tuned by the dopant as well as the charge state of the cluster. Further, the structure of the $TMMg_3^{0,+}$ clusters determines the adsorption site for the first adsorbed H_2 molecule, i.e., the geometry of the $H_2TMMg_3^{0,+}$ adsorption complex. This is crucial for step-wise addition of further H_2 molecules to the $H_2TMMg_3^{0,+}$ complex. A single H_2 molecule interacts with $TMMg_3^{0,+}$ clusters mainly through the TM atoms via charge transfer mechanism as observed from the density of states and donor-acceptor analyses of our computed data. Studies of adsorption complexes with multiple hydrogen molecules signify that all the H_2 compete to interact with the TM atoms/ions of the clusters. Therefore, it is also required for the $TM^{0,+}$ to maintain peripheral positions in the clusters so that they can get exposed to all the H_2 molecules. Apart from this, moderate interaction instead of strong binding with the first H_2 molecule, in fact, can sustain for larger number of hydrogen adsorption in $TMMg_3^{0,+}$ clusters. High symmetric clusters with the $TM^{0,+}$ dopants with higher Mg coordination support strong interaction with the first H_2 molecule and hence get saturated with less number of such molecules. In such clusters, all the coordinated Mg atoms help the $TM^{0,+}$ indirectly to interact with the first H_2 molecule, which become feeble soon in the successive steps. The underlying factors to the strength of cluster-hydrogen interaction are the molecular electrostatic potential surfaces; orientation of molecular orbitals of the cluster with those of H_2 ; donation and back-donation of electronic charges between the cluster and H_2 molecules. Among the clusters considered in our study, two higher energy low symmetrical isomers of $NiMg_3$ and $FeMg_3^+$ clusters are found to adsorb larger number of H_2 molecules than the corresponding lowest energy symmetric ground states. The gravimetric densities of these two isomers are 13.28 wt% and 7.89 wt%, respectively. This study, in near future, will open up new directions in the investigation of suitable hydrogen storage materials for practical applications.

Acknowledgement BB thanks University Grants Commission, India for research fellowship.

References

- [1] <https://www.energy.gov/eere/fuelcells/hydrogen-storage>
- [2] S. K. Bhatia, A. L. Myers, Optimum conditions for adsorptive storage, *Langmuir*. 22 (2006)1688 – 1700.
- [3] R.C. Lochana, M. Head-Gordon, Computational studies of molecular hydrogen binding affinities: the role of dispersion forces, electrostatics and orbital interactions, *Phys. Chem. Chem. Phys.* 8 (2006)1357 – 1370.
- [4] N. Yuksel, A. Kose, M. F. Fellah, A density functional theory study of molecular hydrogen adsorption on Mg site in OFF type zeolite cluster, *Int. J. Hydrogen Energy*. 45 (2020) 34983 – 34992.
- [5] K. Gopalsamy, V. Subramanian, Hydrogen storage capacity of alkali and alkaline earth metal ions doped carbon based materials: A DFT study, *Int. J. Hydrogen Energy*. 39 (2014) 2549 – 2559.
- [6] A. Kumar, N. Vyas, A. K. Ojha, Hydrogen storage in magnesium decorated boron clusters ($Mg_2Bn, n = 4-14$):A density functional theory study, *Int. J. Hydrogen Energy*. 45 (2020) 12961 – 12971.
- [7] K. Srinivasu, S. K. Ghosh, R. Das, S. Giri, P. K. Chattaraj, Theoretical investigation of hydrogen adsorption in all-metal aromatic clusters, *RSC Advances*. 2 (2012) 2914 – 2922.
- [8] B. Boruah, B. Kalita, Exploring enhanced hydrogen adsorption on Ti doped Al nanoclusters: A DFT study, *Chem. Phys.* 518 (2019) 123-133.
- [9] X. B. Xie et al., First principles studies in Mg-based hydrogen storage materials: A review, *Energy*. 211 (2020) 118959.
- [10] X. Wang, L. Andrews, Infrared spectra of magnesium hydride molecules, complexes and solid magnesium hydride, *J. Phys. Chem. A*. 108(2004) 11511 – 11520.
- [11] B. Li et al., Mg-based metastable nano alloys for hydrogen storage, *Int. J. Hydrogen Energy*. 44 (2019) 6007 – 6018.
- [12] V. A. Yartys et. al, Magnesium based materials for hydrogen storage: Past, present and future, *Int. J. Hydrogen Energy*. 44 (2019) 7809 – 7859.
- [13] D. He, Y. Wang, C. Wu, Q. Li, W. Ding, C. Sun, Enhanced hydrogen desorption properties of magnesium hydride by coupling non-metal doping nano-confinement, *Appl. Phys. Lett.* 107 (2015) 243907-1 – 243907-5.

- [14] Z. Sun, X. Lu, F. M. Nyahuma, N. Yan, J. Xiao, S. Su, L. Zhang, Enhancing hydrogen storage properties of MgH_2 by transition metals and carbon materials: A brief review, *Front. Chem.* 8 (2020) 552-1-552 – 552-14.
- [15] W. W. P. Wagemans, J. H. van Lanthe, P.E. de Jongh, A. J. van Dillen, K. P. de Jong, Hydrogen storage in magnesium clusters: Quantum chemical study, *J. Am. Chem. Soc.* 127 (2005) 16675 – 16680.
- [16] I. P. Jain, C. Lal, A. Jain, Hydrogen storage in Mg: A most promising material, *Int. J. Hydrogen Energy.* 35 (2010) 5133 – 5144.
- [17] J. Liu, J. Tyrrell, L. Cheng, Q. Ge, First-principles studies on hydrogen desorption mechanism of Mg_nH_{2n} ($n = 3, 4$), *J. Phys. Chem. C.* 117 (2013) 8099 – 8104.
- [18] W. Ma, C. Jing, First-principles study on hydrogen storage in Al-, Ca-, Mn- doped MgNi clusters, *Int. J. Mod. Phys. B* 31 (2017) 1730002-1 – 1730002-10.
- [19] X. Zhang, Y. Liu, Z. Ren, et al. Realizing 6.7 wt% reversible storage of hydrogen at ambient temperature with non-confined ultrafine magnesium hydrides, *Energy Environ. Sci.* 14 (2021) 2302 – 2313.
- [20] E. N. Kaukaras, A. D. Zdetsis, M. M. Sigalas, Ab initio study of magnesium and magnesium hydride nanoclusters and nanocrystals: Examining optimal structures and compositions of efficient hydrogen storage, *J. Am. Chem. Soc.* 134 (2012) 15914 – 15922.
- [21] N. S. Norberg, T. S. Arthur, S. J. Fredrick, A. L. Prieto, Size dependent hydrogen storage properties of Mg nanocrystals prepared from solution, *J. Am. Chem. Soc.* 133 (2011) 10679 – 10681.
- [22] F. Cheng, Z. Tao, J. Liang, J. Chen, Efficient hydrogen storage with the combination of lightweight Mg/MgH_2 and nanostructures, *Chem. Commun.* 48 (2012) 7334 – 7343.
- [23] K. J. Jeon, H. R. Moon, A. M. Ruminski, B. Jiang, C. Kisielowski, R. Bardhan, J. J. Urban, Air-stable magnesium nanocomposites provide rapid and high-capacity hydrogen storage without using heavy metal catalysts. *Nat. Mater.* 10 (2011) 286 – 290.
- [24] D. Shen, C. P. Kong, R. Jia, P. Fu, H. X. Zhang, Investigation of properties of Mg_n clusters and their hydrogen storage mechanism: A study based on DFT and Global minimum optimisation method, *J. Phys. Chem. A.* 119 (2015) 3636-3643.
- [25] P. Banerjee, K. R. S. Chandrakumar, G. P. Das, Exploring adsorption and desorption characteristics of molecular hydrogen on neutral and charged Mg nanoclusters: A first principles study, *Chem. Phys.* 469-470 (2016)123 – 131.
- [26] A. K. Srivastava, N. Misra, Ab initio investigations on planar $(MgO)_n$ clusters ($n=1-5$) and their hydrogen adsorption behaviour, *Molecular Simulations.* 42(2016):208 – 214.

- [27] M. El Khatabi, M. Bhihi, S. Naji, H. Labrim, A. Benyoussef, A. El kenz, M. loulidi, Study of doping effects with 3d and 4d-transition metals on the hydrogen storage properties of MgH_2 , *Int. J. Hydrogen Energy*. 41(2016):4712 – 4718.
- [28] Y. Wnag, S. Lu, Z. Zhou, G. jin, Z. Lan, Effect of transition metal on hydrogen storage properties of Mg-Al alloy, *J. Mater. Sci.* 52 (2017) 2392 – 2399.
- [29] R. Trivedi, D. Bandyopadhyay, Study of adsorption and dissociation pathway of H_2 molecule on Mg_nRh (n=1-10) clusters: A first principle investigation, *Int. J. Hydrogen Energy*. 41 (2016) 20113 – 20121.
- [30] M. Pozzo, D. Alfe, A. Amieiro, S. French, A. Pratt, Hydrogen dissociation and diffusion on Ni-, Ti- doped Mg(001) surfaces, *J. Chem. Phys.* 128 (2008) 094703-1 – 094703-1-11.
- [31] R. Trivedi, D. Bandyopadhyay, Hydrogen adsorption in small size Mg_nCo clusters: A density functional study, *Int. J. Hydrogen Energy*. 40 (2015;) 12727 – 12735.
- [32] X. Xie, M. Chen, M. Hu, B. Wang, R. Yu, T. Liu, Recent advances in Mg-based hydrogen storage materials with multiple catalysts, *Int. J. Hydrogen Energy*. 44 (2019) 10694 – 10712.
- [33] X. Ma, S. Liu, S. Huang, Hydrogen adsorption and dissociation on the TM-doped (TM=Ti, Nb) Mg_{55} nanoclusters: A DFT study, *Int. J. Hydrogen Energy*. 42 (2017) 24797 – 24810.
- [34] Y. Wu, Y. Meng, L. Ma, J. Zhao, J. Tang, H. Chen, How does Ti-doping effect hydrogen storage properties of MgH_2 at nanosize, *Russ. J. Phys. Chem. A.* 95(2021) 1424 – 1431.
- [35] G. J. Kubas, Metal-dihydrogen and σ -bond coordination: the consummate extension of the Dewar-Chatt-Duncanson model for metal olefin π -bonding, *J. Organ. Chem.* 635 (2001) 36 – 68.
- [36] M. Jia, J. Vanbuel, P. Ferrari, E. M. Fernandez, S. Gewinner, W. Schollkopf, M. T. Nguyen, A. Fielicke, E. Jenssens, Size dependent H_2 adsorption on Al_nRh^+ (n=1-12) clusters, *J. Phys. Chem. A.* 122 (2018) 18247 – 18255.
- [37] M. Jia, J. Vanbuel, P. Ferrari, W. Schollkopf, A. Fielicke, M. T. Nguyen, E. Jenssens, Hydrogen adsorption and dissociation Al_nRh^{2+} (n=1-9) clusters: Steric and coordination effect, *J. Phys. Chem. C.* 124 (2020) 7624 – 7633.
- [38] C. He, H. L. Chen, Y. Sheng, First-principles study of molecular hydrogen adsorption on Mg_nZr (n = 1 – 11) clusters, *Eur. Phys. J. D.* 73 (2019) 90-1 – 90-8.
- [39] A. Ozkanlar, A. Samuels, A. E. Clark, Modulation of hydride formation energies in transition metal doped Mg by alternation of spin state, *Chem. Phys. Lett.* 560 (2013) 10 – 14.

- [40] D. Moser, D. J. Bull, T. Sato, et al., Structure and synthesis of high pressure synthesized Mg-TM hydrides (TM= Ti, Zr, Hf, V, Nb and Ta) as possible new hydrogen rich hydrides for hydrogen storage, *J. Mater. Chem.* 19 (2009) 8150 – 8161.
- [41] L. Xie, Y. Liu, X. Zhang, J. Qu, Y. Wang, X. Li, Catalytic effect of Ni nanoparticles on the desorption kinetics of MgH_2 nanoparticles, *J. Alloy. Compd.* 482 (2009) 388 – 392.
- [42] J. Cui, J. Liu, H. Wang, L. Ouyang, D. Sun, M. Zhu, et al., Mg-TM (TM: Ti, Nb, V, Co, Mo or Ni) core-shell like nanostructures: synthesis, hydrogen adsorption performance and catalytic mechanism, *J. Mater. Chem. A.* 2 (2014) 9645 – 9655.
- [43] A. P. Maltsev, O.P. Charkin, Theoretical modelling of stepwise addition of H_2 molecules to magnesium clusters Mg_{18} and $Mg_{17}M$, *Russ. J. Inorg. Chem.* 65 (2020) 185 – 192.
- [44] A. P. Maltsev, O.P. Charkin, Theoretical modelling of stepwise addition of H_2 molecules to $Mg_{17}L$ magnesium clusters doped with 3d metals, *Russ. J. Inorg. Chem.* 65 (2020) 1204 –
- [45] O.P. Charkin, A. P. Maltsev, Density functional theory modelling of reactions of addition of H_2 molecules to magnesium clusters $Mg_{17}M$ doped with atoms M of transition 3d elements, *J. Phys. Chem. A.* 125 (2021) 2308 – 2315.
- [46] Gaussian 09, Revision D.01, Frisch MJ, Trucks GW, Schlegel HB, Scuseria GE, Robb MA, Cheeseman JR, Scalmani G, Barone V, Mennucci B, Petersson GA, et al. Gaussian, Inc., Wallingford CT, 2009.
- [47] B. Boruah, B. Kalita, Role of transition metal doping in determining the electronic structure and properties of small magnesium clusters: a DFT-based comparison of neutral and cationic states, *J. Nanopart. Res.* 22 (2020) 370-1 – 370-19.
- [48] J. D. Chai, M. H. Gordon, Long-range corrected hybrid density functionals with damped atom-atom dispersion corrections, *Phys. Chem. Chem. Phys.* 10 (2008) 6615 – 6620.
- [49] Y. Minekov, A. Singstad, G. Occhipinti, V. R. Jensen, The accuracy of DFT-optimised geometries of functional transition metal compounds: a validation study of catalysts for olefin metathesis and other reactions in the homogeneous phase, *Dalton Trans.* 41 (2012) 5526 – 5541.
- [50] T. Lu, F. Chen, Multifwfn: A multifunctional wavefunction analyzer, *J. Comput. Chem.* 33 (2012) 580-592.